Observation of Ultraslow and Stored Light Pulses in a Solid

A. V. Turukhin,* V. S. Sudarshanam, and M. S. Shahriar
Research Laboratory of Electronics, Massachusetts Institute of Technology, 77 Massachusetts Avenue, Cambridge, Massachusetts 02139

J. A. Musser
Texas A&M University, College Station, Texas 77843

B. S. Ham
Center for Quantum Coherence and Communications, Electronics and Telecommunications Research Institute, Daejon 305-350, South Korea

P. R. Hemmer
Air Force Research Laboratory, Sensors Directorate, Hanscom AFB, Massachusetts 01731
(Received 7 December 2000; revised manuscript received 15 August 2001; published 20 December 2001)

We report ultraslow group velocities of light in an optically dense crystal of Pr doped Y_2SiO_5. Light speeds as slow as 45 m/s were observed, corresponding to a group delay of 66 μs. Deceleration and "stopping" or trapping of the light pulse was also observed. These reductions of the group velocity are accomplished by using a sharp spectral feature in absorption and dispersion that is produced by resonance Raman excitation of a ground-state spin coherence.

DOI: 10.1103/PhysRevLett.88.023602 PACS numbers: 42.50.Gy, 42.62.Fi

Since the first observations of ultraslow light [1,2], there has been substantial interest in its potential applications. For example, it was proposed that slowing the group velocity of a laser pulse down to the speed of sound in a material can produce strong coupling between acoustic waves and the electromagnetic field [3]. This might be utilized for efficient multiwave mixing and quantum nondemolition measurements [4], as well as for novel acousto-optical devices. Ultraslow light might even allow nonlinear interactions down to a single photon level [5]. Finally, it has been suggested [6] and experimentally demonstrated [7,8] that the group velocity of light can be decelerated to zero, effectively trapping or "stopping" the light pulse. Light stored by this technique is potentially important for quantum computing applications because it is relatively easy to implement and can be accomplished with near 100% fidelity in principle.

For many potential applications of slow light, a solid-state medium is preferred. However, most solid materials have relatively broad optical linewidths, which limits the achievable light-speed reduction. A notable exception to this general rule is a class of materials consisting of rare-earth doped insulators that exhibit spectral hole burning [9]. These materials are generally used for ultrahigh density optical memories and processors [10]. In one such material, Pr doped Y_2SiO_5 (Pr:YSO) [11], efficient, narrow-linewidth electromagnetically induced transparency (EIT) [12] has also been demonstrated [13]. This is significant because narrow band EIT enabled the demonstration of ultraslow and "stopped" light in atomic vapors.

In this Letter, we demonstrate ultraslow group velocities and the storage or "stopping" of light pulses in a Pr:YSO crystal. Our crystal was supplied by Scientific Materials, Inc., and consists of 0.05 at. % Pr. It has a thickness of 3 mm in the light propagation direction and both entrance and exit faces are polished and antireflection coated. The laser setup is similar to that described in Ref. [13]. Briefly, acousto-optic frequency shifters are used to generate the required laser frequencies from the output of a single dye laser. The laser beams are focused to a diameter of $\sim$100 μm (FWHM) in the crystal and intersect at angles in the range of 10–20 mrad. All beams are linearly polarized along the crystal axis that gives maximum absorption. The 606 nm optical transition [11] at site 1 in Pr:YSO is used, where the relevant (Kramer's degenerate) spin sublevels are depicted in Fig. 1(a). Here, the coupling and the probe fields are denoted by frequencies ω_C and ω_P, respectively. Because of the long population lifetime of the ground state sublevels, more than 100 sec at our 5 K operating temperature, the crystal soon becomes transparent to these laser fields because of optical pumping, as illustrated by the solid curve in Fig. 1(b), thereby preventing further absorption and EIT. The width of this transparency or "spectral hole" is determined by the spectral widths, intensities, and interaction times of the coupling and probe fields.

To counteract the spectral hole burning effect and provide a high optical density for EIT, an auxiliary or repump field ω_A is also needed, as shown in Fig. 1(a). This auxiliary field creates an absorbing "antihole" near the center of the hole bleached by the coupling and probe fields, as shown by the dotted curves in Fig. 1(b). The width of this antihole is determined by both laser jitter and the spin inhomogeneous width, and its peak absorption is

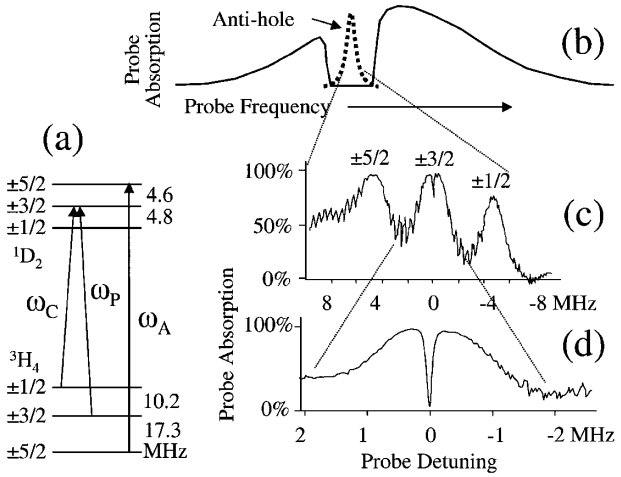

FIG. 1. (a) Energy level diagram for Pr:YSO. Coupling field: ω_C, probe field: ω_P, and auxiliary field: ω_A. (b) Schematic representation of hole burning in the inhomogeneous optical absorption line (solid curve) and an antihole created by the auxiliary field (dotted curve). (c) Observed antihole absorption with excited-state components labeled. (d) Extended scan of the central antihole showing near 100% efficient EIT. Intensities are coupling = 470 W/cm^2, probe = 1.1 W/cm^2, auxiliary = 47 W/cm^2.

determined by the auxiliary beam intensity. The intensity of the auxiliary field therefore controls the effective probe absorption (weak probe limit) much the same as varying the atomic density controls the absorption in a vapor. More importantly, the antihole width determines the effective inhomogeneous linewidth that must be overcome by the Rabi frequency of the coupling field to establish efficient EIT. In our experiments, laser jitter on the scale of 1–2 MHz dominates this antihole width, but if a highly stable laser were used, antihole widths of less than 100 kHz should be possible. Since these widths are much smaller than the 4.4 GHz intrinsic inhomogeneous width of the optical transition, efficient EIT can be established at a much lower coupling intensity than would otherwise be predicted. Because of this narrow effective inhomogeneous linewidth, the doped crystal more closely resembles an ultracold vapor than a warm vapor. The absence of atomic motion, and therefore Doppler shifts and diffusion, is also an advantage that the crystal and ultracold vapor share.

A typical antihole pattern is shown in Fig. 1(c). Note that there are three absorption peaks due to the multiple excited state sublevels. Laser jitter is responsible for the noise and the lack of fully resolved peaks in the data shown. A narrow, EIT dip in absorption is visible in the central antihole. For a sufficiently strong coupling laser, the induced transparency can approach 100% as shown in Fig. 1(d). Although power broadened, the measured EIT linewidth in this trace is within a factor of 2 of the inhomogeneous linewidth of the ground-state spin transition, as measured by optically detected nuclear magnetic resonance (ODNMR) [14].

To measure group velocity, the probe is chopped and its phase delay is measured using a lock-in amplifier, as described in previous slow light experiments [2]. Group delays greater than 65 μsec are observed, as shown in Fig. 2(a), which correspond to light group velocities as slow as ~45 m/s [see Fig. 2(b)] for the 3 mm long crystal. The observed delays are found to be independent of the probe modulation frequency (measured over the range of 3–6 kHz), as required.

We also investigated the slowing of individual probe pulses. Figure 2(c) shows probe pulse delays for various two-photon detunings from the center of the EIT dip, with the detunings illustrated graphically by the vertical dotted lines in the inset. As expected, the observed group delay is very sensitive to detuning from the transparency condition. On resonance, a maximum delay of about 100 μsec is measured from the center of the input pulse to the center of the delayed pulse. This is comparable to the delays

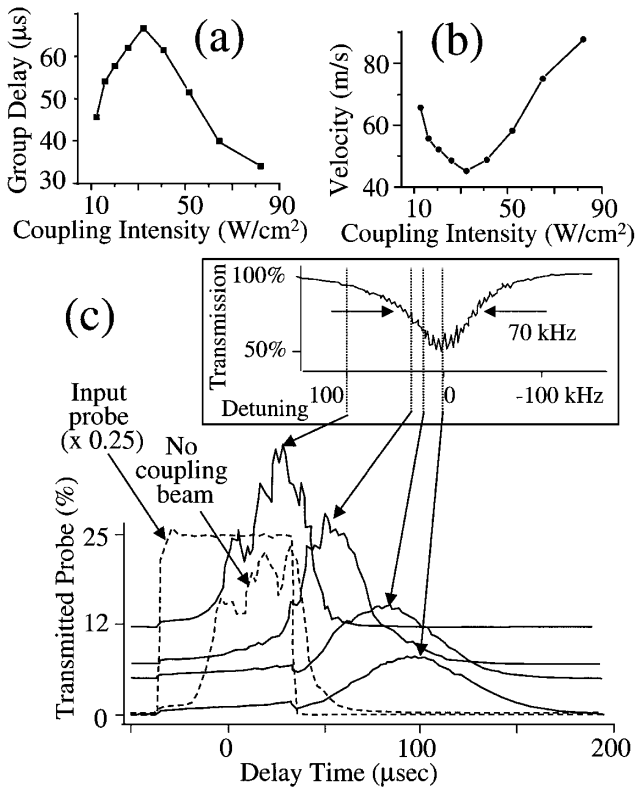

FIG. 2. Slow light demonstration. (a) Measured group delay vs coupling beam intensity. Coupling intensities as labeled, probe = 0.13 W/cm^2, auxiliary = 1.8 W/cm^2. Coupling and auxiliary are cw, probe is chopped with 50% duty cycle. (b) Deduced group velocity of light vs coupling beam intensity. (c) Slowed probe light for several detunings from the center of the EIT resonance. Detunings are 0, 20, 30, and 100 kHz. The inset shows the approximate detunings superimposed on a representative EIT dip. For reference, dashed traces show the input probe, and the transmitted probe in the absence of a coupling beam. Probe pulse duration = 70 μsec. Intensities are the following: coupling = 77 W/cm^2, probe = 5.5 W/cm^2, auxiliary = 120 W/cm^2. For state preparation, first the coupling and then the auxiliary fields are turned on for 10 ms each, followed by a 1 msec dark time. The coupling field is again turned on 200 μsec prior to the probe pulse. All traces are averaged over 10 shots.

measured by the modulation technique [Fig. 2(a)]. Note that even for a two-photon detuning as small as 100 kHz, the delays are greatly reduced, becoming comparable to those seen in the absence of the coupling field, as illustrated by the dashed traces in Fig. 2(c). The fact that a probe pulse delay is still seen in the absence of the coupling field is due to the high probe intensity that was used in the pulsed experiments to overcome noise due to scattered light from the coupling laser. At such high probe intensities, self-induced transparency [15] (SIT) is expected because the probe Rabi frequency is comparable to the excited state lifetime (homogeneous $T_2 = 111$ μsec and population $T_1 = 152$ μsec) [16].

One of the key advantages of light slowed by EIT-enhanced dispersion, compared to an absorption-based process like SIT, is that the EIT-produced group delays depend primarily on the coupling laser intensity, rather than the probe intensity. This implies that EIT can slow complex probe pulse shapes, subject only to its bandwidth limitations. Another advantage of EIT is the ability to manipulate the group light speed via changes in the coupling laser intensity. These capabilities are illustrated in Fig. 3(a), which shows the acceleration of a slowed light pulse. In this demonstration, light is initially slowed using approximately the same coupling beam intensity as in Fig. 2(c), but then the coupling intensity is suddenly increased. This increase occurs at progressively earlier times going from top to bottom as illustrated by the dashed lines superimposed on the data. As expected, the probe delay is correspondingly shorter, since the increase in coupling field strength causes light speedup due to power broadening. In the topmost trace, the coupling field is not increased until after the slowed probe has emerged from the crystal, and the result is nearly identical to the resonant case of Fig. 2(c). In the bottom-most trace, the coupling intensity is increased before the probe is input. The delay is significantly less and the transmitted pulse more closely resembles the square input probe pulse. This is because the wider bandwidth of the power broadened EIT not only gives a faster group velocity, but also passes more of the Fourier components that give rise to the sharp edges. In contrast, the second trace from the bottom corresponds to an increase in coupling intensity after the slowed probe pulse has entered the crystal, but before it has emerged. This trace has a width, shape, and height that are consistent with a time-compressed version of the slowed pulse in the top trace, which demonstrates that the light speed is manipulated while the probe pulse is propagating inside the crystal.

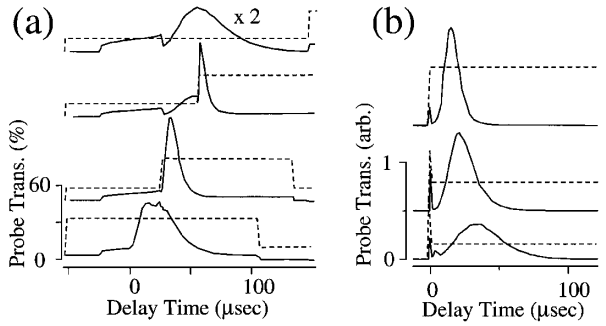

FIG. 3. Light acceleration and deceleration demonstrations. (a) Light pulses acceleration produced by increasing the coupling intensity as illustrated by accompanying dashed lines. The top trace is similar to the resonant case of Fig. 2(c). The coupling intensity is increased while (second trace), and before (third trace) the slowed pulse exits the crystal. For comparison, the bottom trace shows the slow light when the coupling intensity is increased before the probe enters the crystal. The remaining experimental conditions are similar to those in Fig. 2(c). The probe pulse duration = 50 μsec. Intensities are the following: strong coupling = 535 W/cm^2, weak coupling = 77 W/cm^2, auxiliary = 60 W/cm^2. (b) Decelerated slow light produced by decreasing the coupling intensity to 54% (middle trace) and 28% (bottom trace) of its initial value. For reference, the top trace shows the slow light when the coupling intensity is not decreased. The input probe pulse duration = 3 μsec. Intensities are as follows: strongest coupling = 543 W/cm^2, probe = 373 W/cm^2, auxiliary = 95 W/cm^2.

In addition to acceleration, slow light can also be decelerated as shown in Fig. 3(b). Here, light is initially slowed using a strong coupling laser (top trace), and then decelerated by decreasing the coupling intensity, as illustrated by the dashed lines, while the pulse is inside the crystal (bottom two traces).

Finally, as mentioned before, one of the potentially most important applications of slow light is in quantum information storage via trapped or "stopped" light [6]. This is accomplished by decelerating the probe pulse to zero velocity via reducing the coupling laser intensity to zero. The stored pulse is then retrieved at a later time by restoring the coupling laser. Storage by trapped light is demonstrated in Fig. 4. Here, Fig. 4(a) shows a reference slow light pulse taken under conditions similar to those of Figs. 2(c) and 3(a). It should be noted that the complex pulse shape in this and, to a lesser extent, in the previous figures is due to the fact that both slow and fast light components of the probe are transmitted by the crystal. The fast component, which emerges first and preserves the square input pulse shape is present because the probe absorption is only about 95% for the auxiliary beam intensity used. In Fig. 4(b) the coupling intensity is reduced to zero while the probe pulse is propagating inside the crystal, as indicated by the dashed line, effectively reducing its propagation velocity to zero. As expected, the slow pulse no longer exits the crystal, but can be recovered at a later time by switching the coupling laser back, as shown, thereby completing the "stopped" light demonstration.

The sharp spike in the output probe beam that appears as soon as the coupling laser is restored is due to a Raman excited spin echo [17] of the transient produced earlier when the coupling laser was suddenly switched off. This transient lies outside the EIT bandwidth and propagates as fast light. Thus, the data provides an experimental comparison of Raman spin echo storage and trapped light storage schemes. The (attenuated) sharp spike in the center

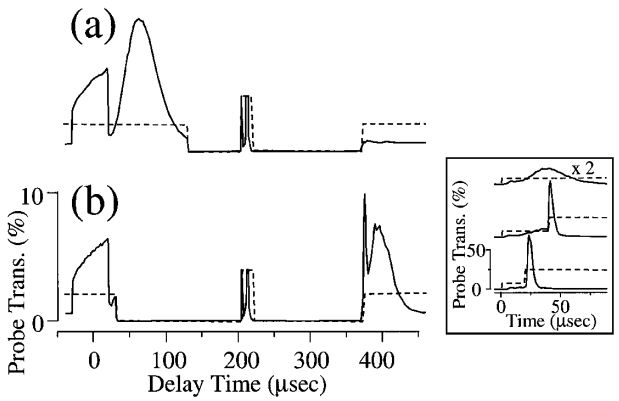

FIG. 4. Light "stopping" demonstration. (a) Reference slow light pulse similar to that in Fig. 3(a). See text for details. (b) Propagation of slow pulse is interrupted or "stopped" by temporarily switching off the coupling laser, as illustrated by the dashed lines. The inset shows the acceleration of the recovered slow light pulse in analogy to Fig. 3(a). The spike (attenuated) in the center of both traces, (a) and (b), is due to a rephrasing pulse. Input probe pulse duration = 50 μsec. Intensities are as follows: coupling = 77 W/cm^2, probe = 11 W/cm^2, auxiliary = 60 W/cm^2. For rephrasing pulse, duration = 7 μsec; intensities are as follows: coupling = 535 W/cm^2; probe = 430 W/cm^2.

of both these traces is due to a rephasing pulse that is required, in a solid, to reverse the dephasing effects of the inhomogeneously broadened spin transition. Finally, the recovered signals are found to decrease in amplitude when storage time is increased, as expected for the 500 μsec spin homogenous lifetime.

To verify that the delayed probe pulse emerging after the coupling laser is restored is actually slow light, the acceleration demonstration of Fig. 3(a) is repeated on the recovered signal in Fig. 4(b) (see inset). Clearly the results are qualitatively the same, verifying that the delayed echo pulse is slow light (i.e., recovered trapped light). For quantum storage applications, it is important to note that trapped light storage is capable of storing not only the magnitude of the input probe field, but also its phase [18]. A similar phase storage capability has already been demonstrated for Raman excited spin echoes [19].

In summary, we demonstrate ultraslow (subsonic) light group velocities, and stopped or trapped light storage in a solid. These observations are key, enabling steps toward many potential applications of slow and trapped light to low-intensity nonlinear optics, quantum information processing, and quantum information storage.

We acknowledge discussions with S. Ezekiel of MIT and S. Yelin of Harvard, and technical support from Mr. John Kierstead. This study was supported by AFRL/SNHC (Contract No. F19628-00-C-0074), ARO Grants No. DAAG55-98-1-0375, AFOSR Grants No. F49620-98-1-0313 and No. F49620-99-1-0224, and the Creative Research Initiative Program of Korean Ministry of Science and Technology.

*Corresponding author.
Email address: alexey.turukhin@us.jdsuniphase.com
Current address: JDS Uniphase Corporation, Optical Networks Research, 625 Industrial Way West, Eatontown, NJ 07724.

[1] L. V. Hau, S. E. Harris, Z. Dutton, and C. Behroozi, Nature (London) **397**, 594 (1999).
[2] M. Kash, V. Sautenkov, A. Zibrov, L. Hollberg, G. Welch, M. Kukin, Y. Rostovsev, E. Fry, and M. Scully, Phys. Rev. Lett. **82**, 5229 (1999).
[3] A. Matsko, Y. Rostovtsev, H. Cummins, and M. Scully, Phys. Rev. Lett. **84**, 5752 (2000).
[4] V. Braginsky and F. Khalili, *Quantum Measurement* (Cambridge University Press, Cambridge, United Kingdom, 1992).
[5] M. Lukin and A. Imamoglu, Phys. Rev. Lett. **84**, 1419 (2000).
[6] M. Fleischhauer and M. D. Lukin, Phys. Rev. Lett. **84**, 5094 (2000).
[7] C. Liu, Z. Dutton, C. H. Behroozi, and L. V. Hau, Nature (London) **409**, 490 (2001).
[8] D. F. Phillips, A. Fleischhauer, A. Mair, R. L. Walsworth, and M. D. Lukin, Phys. Rev. Lett. **86**, 783 (2001).
[9] R. M. MacFarlane and R. M. Shelby, *Coherent Transients and Holeburning Spectroscopy of Rare Earth Solids,* Spectroscopy of Solids Containing Rare Earth Ions, edited by A. A. Kaplyanskii and R. M. MacFarlane (Elsevier Science Publishers, New York, 1987), Chap. 3.
[10] H. Lin, T. Wang, and T. W. Mossberg, Opt. Lett. **20**, 1658 (1995); X. A. Shen and R. Kachru, Opt. Lett. **20**, 2508 (1995); B. S. Ham, M. K. Kim, P. R. Hemmer, and M. S. Shahriar, Opt. Lett. **22**, 1849 (1997).
[11] R. W. Equall, R. L. Cone, and R. M. Macfarlane, Phys. Rev. B **52**, 3963 (1995); K. Holliday, M. Croci, E. Vauthey, and U. P. Wild, Phys. Rev. B **47**, 14 741 (1993).
[12] S. E. Harris, Phys. Today **50**, No. 7, 36 (1997).
[13] B. Ham, P. Hemmer, and M. Shahriar, Opt. Commun. **144**, 227 (1997).
[14] L. E. Erickson, Opt. Commun. **21**, 147 (1977).
[15] S. L. McCall and E. L. Hahn, Phys. Rev. Lett. **18**, 908 (1967); L. Allen and J. H. Eberly, *Optical Resonance and Two Level Atoms* (Wiley, New York, 1975).
[16] G. Zumofen, F. R. Graf, A. Renn, and U. P. Wild, J. Lumin. **83–84**, 379 (1999).
[17] B. S. Ham, M. K. Kim, P. R. Hemmer, and M. S. Shahriar, Opt. Lett. **22**, 1849 (1997).
[18] A. Mair, J. Hager, D. F. Phillips, R. L. Walsworth, and M. D. Lukin, quant-ph/0108046.
[19] P. R. Hemmer, K. Z. Cheng, J. Kierstead, M. S. Shahriar, and M. K. Kim, Opt. Lett. **19**, 296 (1994).